Data Analysis and Boron Isotope Identification with the AMS-02 on the ISS

LIP Summer Internship 2026

Dinis Cruz & João Nunes

Supervisor: Professor Fernando Barão

LABORATÓRIO DE INSTRUMENTAÇÃO
E FÍSICA EXPERIMENTAL DE PARTÍCULAS

Dinis Cruz

- **Degree:** BSc in Physical Engineering (NOVA FCT)
- **Year:** 2nd Year
- **Areas of Interest:** Physics, Artificial Intelligence & Machine Learning
- **Motivation:** Wanted to experience working in this research field, driven by a strong interest in LIP, while actively exploring multiple scientific areas to find a career path.

João Nunes

- **Degree:** BSc in Physics (FCUL)
- **Year:** 2nd Year
- **Areas of Interest:** Physics & Mathematics
- **Motivation:** Wanted to experience what is like to do research, and wanted to learn more about the AMS experiment and the methods used.

The AMS-02 Experiment

Platform: High-energy physics detector aboard the ISS (since 2011).

Key Observables: Precision measurement of cosmic-ray flux, charge (Z), and rigidity (P).

Primary Mission: Understanding particle acceleration, origins, and propagation throughout the Galaxy.

Fundamental Physics: Searches for dark matter signatures, primordial antimatter, and isotopic composition.

Our goal

Framework Development: Build a comprehensive Monte Carlo simulation pipeline to model the measurement chain and instrumental response of the AMS-02 spectrometer for Boron isotopes.

Detector Performance & Resolution Modeling: Replicate the measurement constraints of the Silicon Tracker, Time-of-Flight (TOF), and RICH subsystems to identify and quantify the primary systematic uncertainties governing mass reconstruction.

Data Architecture: Structure the generated kinematic samples and instrumental observables into optimized ROOT TTree structures for downstream cross-validation and statistical fitting.

Statistical Isotopic Separation: Transition from raw observables to reconstructed invariant mass, generating continuous theoretical mass templates to accurately resolve the high-energy isotopic overlap via likelihood estimation.

The AMS-02 Detector

$$m = \frac{ZP}{\gamma\beta}$$

Target: Secondary Cosmic Rays (Boron).

Tracker: Rigidity $(P = \frac{pc}{Ze})$.

Time of Flight and Trigger (TOF)

Ring Imaging Cherenkov (RICH) $\cos(\theta_C) = \frac{1}{\beta n}$

Transition Radiation Detector (TRD): Distinguishes matter particles from antimatter.

Electromagnetic Calorimeter (ECAL): Measures the total energy of the particles

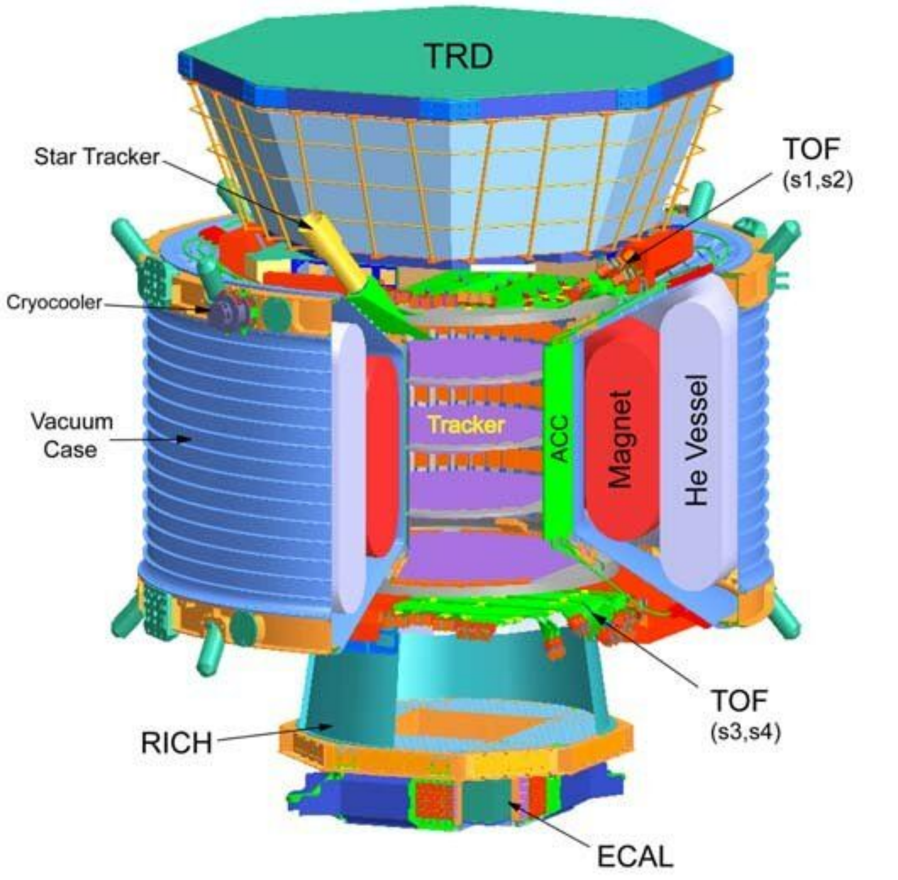

Monte Carlo Simulation

To each particle generated were associated a set of “true” variables randomly generated such as:

- ➔ Mass;
- ➔ Velocity(β);
- ➔ Zenith angle(θ), Azimuthal angle (Φ);
- ➔ x,y variables;
- ➔ Trigger (boolean variable);
- ➔ statistical weight (ω).

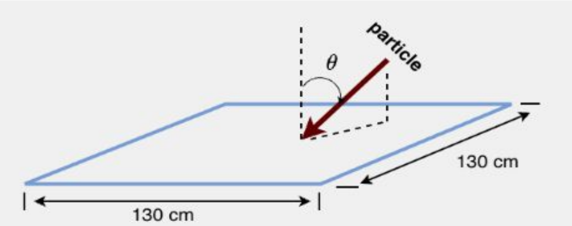

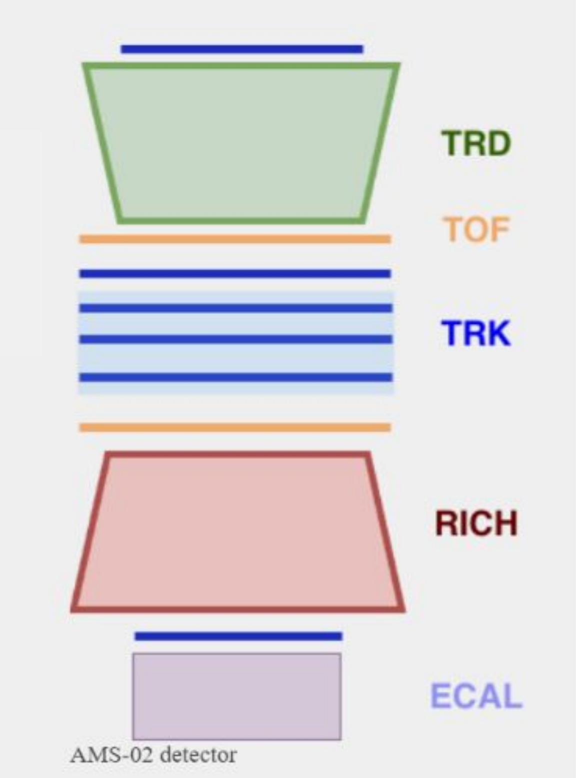

Monte Carlo Simulation - Particle Spectrum

In first approximation, the particle flux is proportional to $P^{-2.7}$, meaning that generating rigidities uniformly across the entire kinematic range would result in a severe statistical deficit at low rigidities and a computational excess at high rigidities, undermining the precision of the Monte Carlo integration. To mitigate this, rigidities were sampled from a log-uniform distribution, ensuring that each momentum decade is populated with an equal number of simulated events.

To reconcile this log-uniform generation with the physical cosmic ray spectrum, a statistical weight ω must be applied to each event.

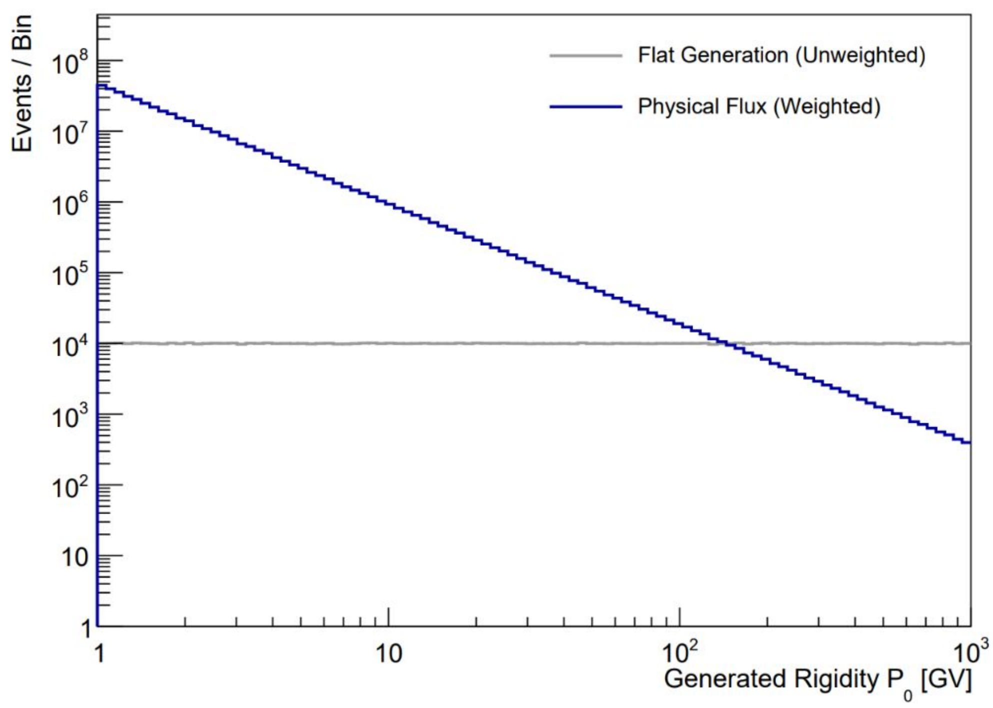

Monte Carlo Simulation - Smearing

A set of smeared particles was also incorporated, representing the values that each subsystem measures during the simulation:

velocity measured with TOF;

$$\beta_{TOF} = \frac{L}{c\left(\frac{L}{c\beta_0} + \sigma_t \cdot \mathcal{N}(0,1)\right)}$$

velocity measured with RICH;

$$\frac{\sigma_{RICH}}{\beta_0} = A - B \cdot \exp\left(1 - \frac{E_{kn}}{E_0}\right)$$

$$\beta_{RICH} = \beta_0 + \beta_0 \left[A - B \cdot \exp\left(1 - \frac{E_{kn}}{E_0}\right)\right] \cdot \mathcal{N}(0,1)$$

rigidity measured with Tracker;

$$P = P_0 + \sigma_P \cdot \mathcal{N}(0,1)$$

reconstructed mass associated to TOF;

reconstructed mass associated to RICH.

Instrumental Resolution

Validation: Ideal $y = x$ kinematic correlation.

Visible the wider range of TOF's measurement.

RICH more accurate and precise.

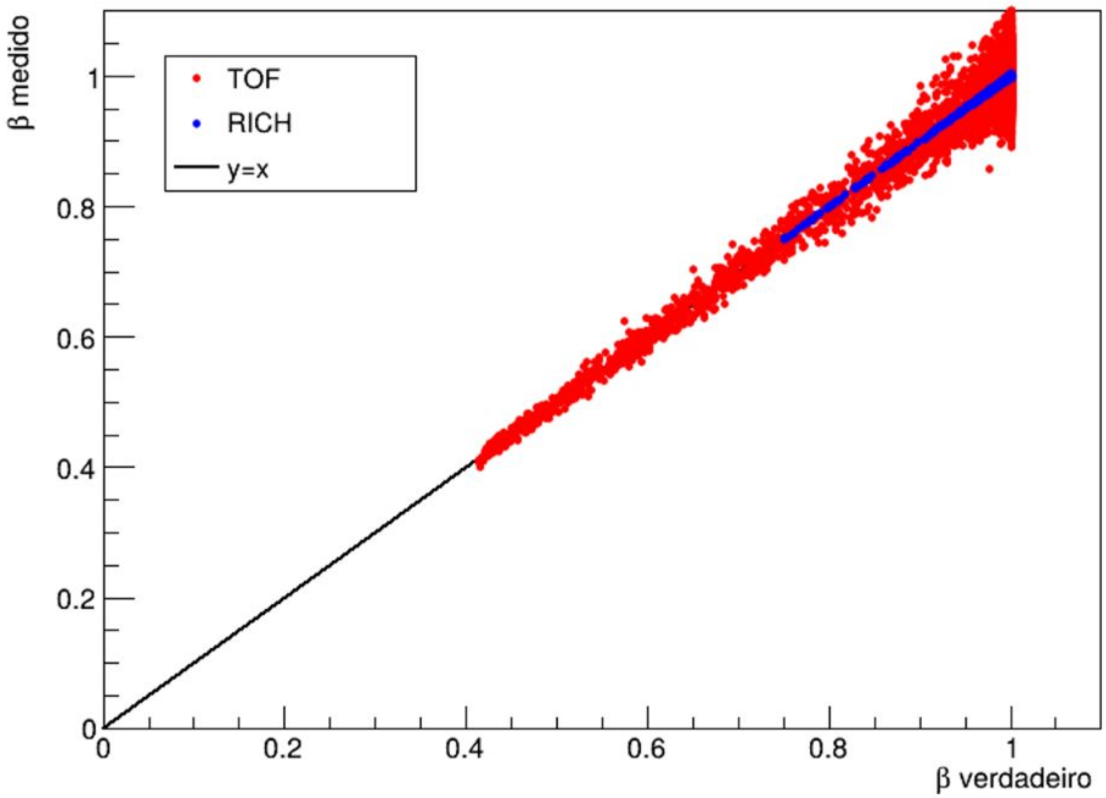

Geometric Acceptance - Spatial Uniform Generation

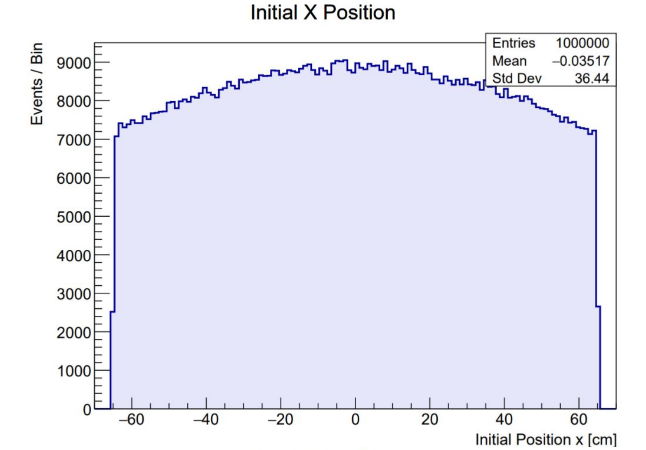

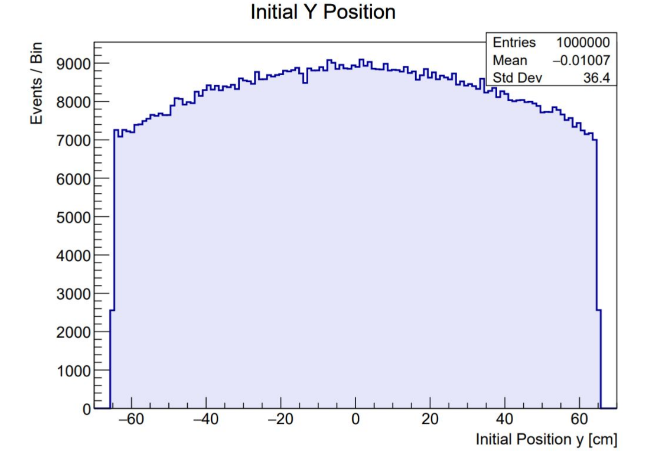

TOF Acceptance:
Dual-plane coincidence trigger requirement ($130 \times 130\ \mathrm{cm}^2$).

Peripheral drop caused by restricted solid angle at detector boundaries.

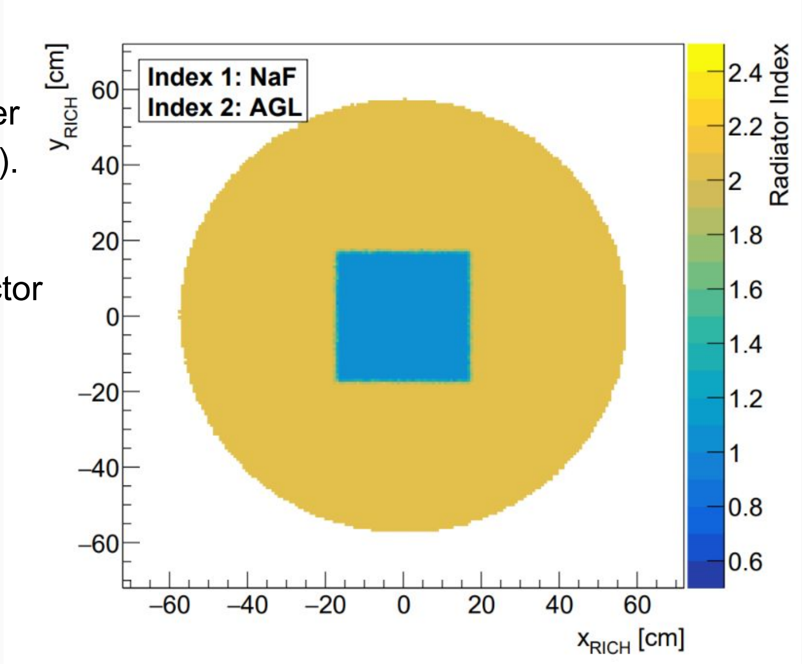

RICH Geometry:
Dual-radiator segregation dictates distinct Cherenkov thresholds ($\beta \geq 1/n$).

Central NaF square: $n = 1.334 \implies \beta \geq 0.750$

Outer AGL ring: $n = 1.050 \implies \beta \geq 0.953$

Geometric Acceptance - Angular Data

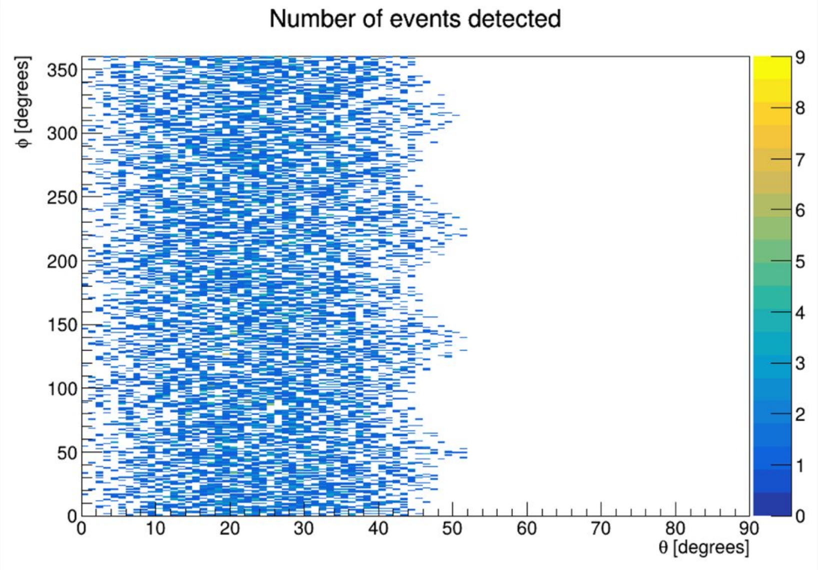

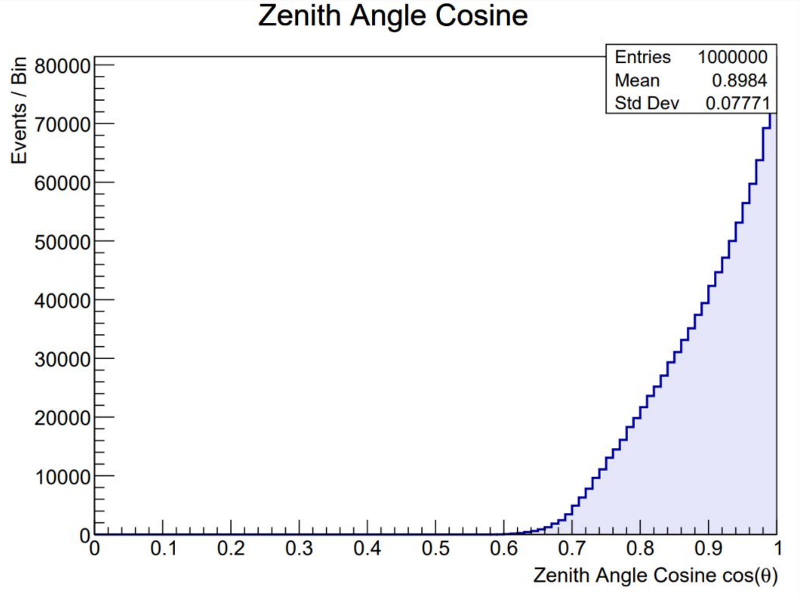

Dual-Plane Trigger: Only events intersecting both upper and lower TOF planes are accepted.
Angular Phase Space: Uniform azimuthal symmetry (ϕ), with the zenith angle (θ) strictly bounded by the detector's physical acceptance cone.
Incidence Profile: Expected event density peak at $\cos(\theta) \approx 1$, confirming the dominance of near-vertical trajectories.

The Kinematic Challenge

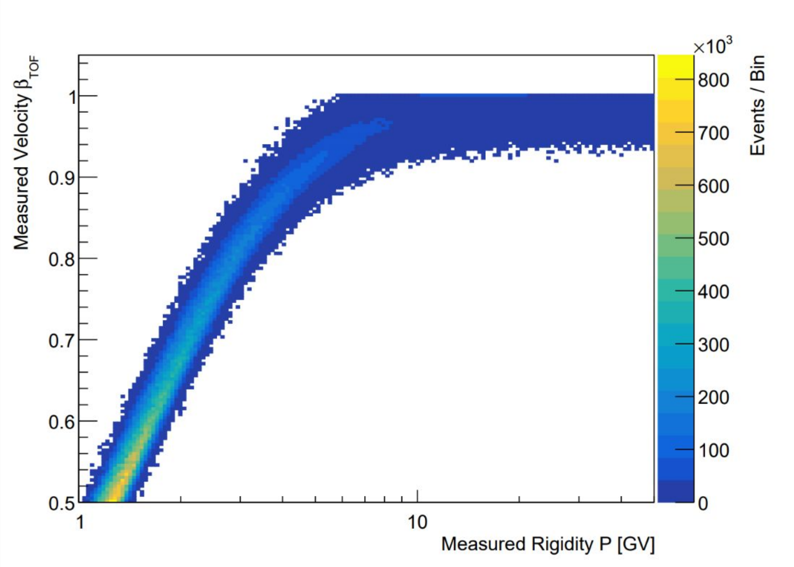

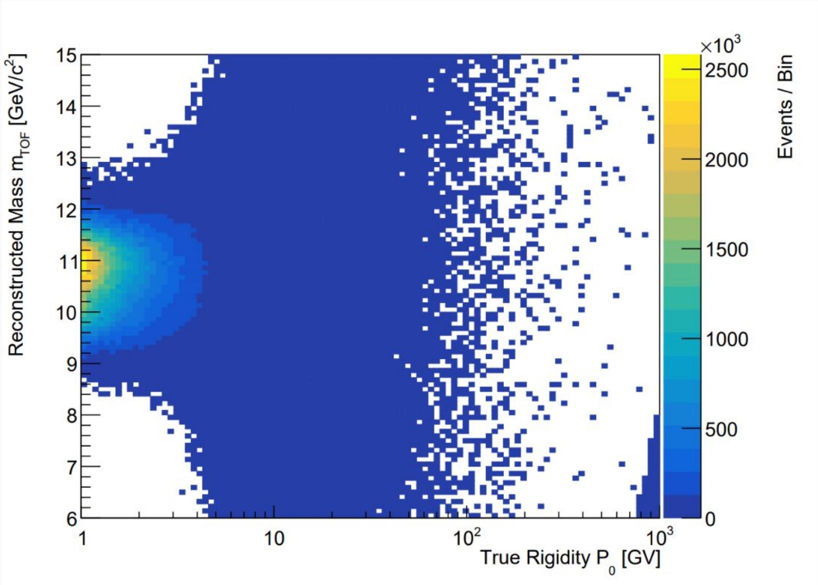

Kinematic Saturation (Left):

- At low energies, distinct isotopic bands are distinguishable.
- As energy increases, velocity asymptotically saturates ($\beta \to 1$), compressing phase space.

Mass Degradation (Right):

- Error propagation ($\delta m/m \approx -\gamma^2 \delta\beta/\beta$) causes severe mass broadening.
- Isotopic mass bands merge into a single continuous distribution above $\sim 10\ \mathrm{GV}$.

Isotopic Mass Overlap

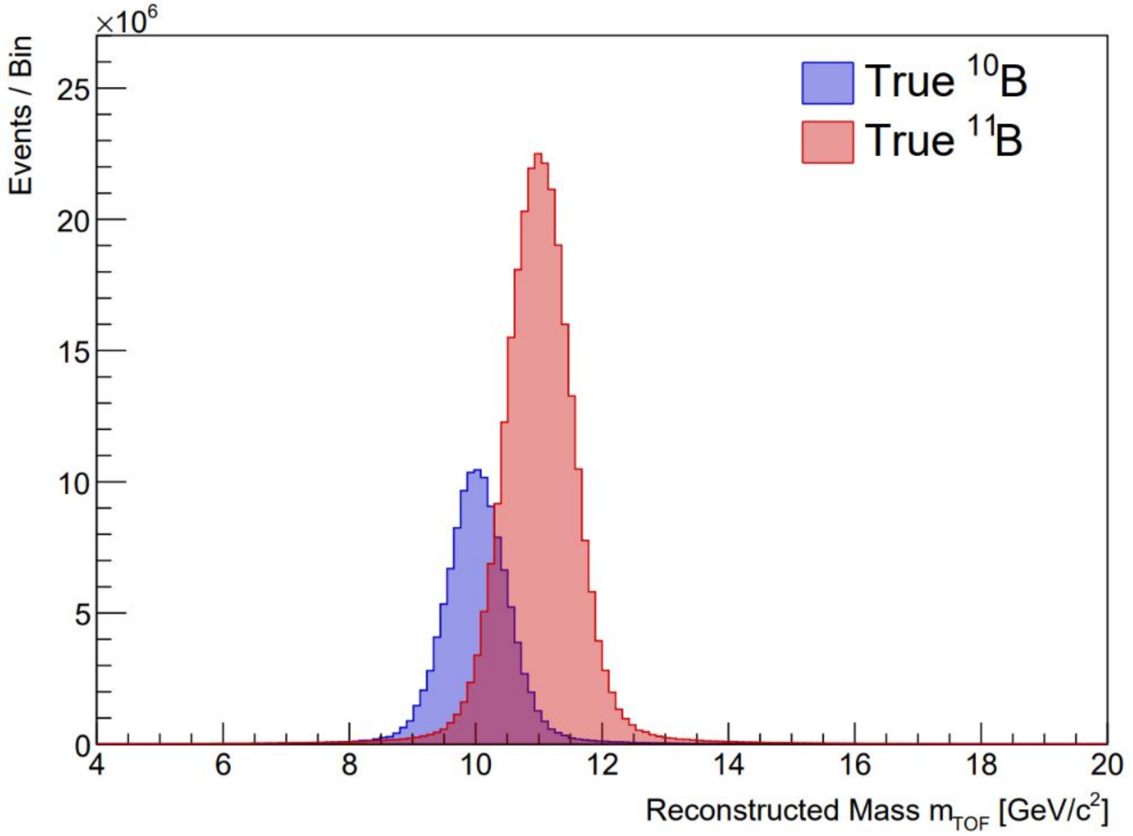

Monte Carlo Truth: Visualizing the physical separation between $^{10}\mathrm{B}$ and $^{11}\mathrm{B}$ that is hidden in real data.

Severe Signal Overlap: Integrated TOF resolution creates cross-contamination, which worsens as $\beta \to 1$.

Non-Gaussian Tails: Non-linear relativistic error propagation and flux drop ($P^{-2.7}$) invalidate Gaussian fits.

Solution: Requires superior RICH velocity resolution combined with continuous Bayesian templates.

Analytical Mass Templates

First-Principles Templates: Continuous PDFs derived via Bayesian numerical integration of instrumental resolutions over the $P^{-2.7}$ flux.

Radiator Isolation $(0.76 < \beta < 0.78)$: Evaluated strictly below the Aerogel Cherenkov threshold $(\beta < 0.953)$ to isolate NaF.

Morphological Asymmetry:

- At fixed β, the heavier $^{11}\mathrm{B}$ demands higher rigidity.
- Linear error scaling ($\sigma_P = 0.04P$) broadens
- the $^{11}\mathrm{B}$ distribution.
- Unit area normalization inherently suppresses
- its peak amplitude. $\int \frac{dN}{dm} dm = 1$

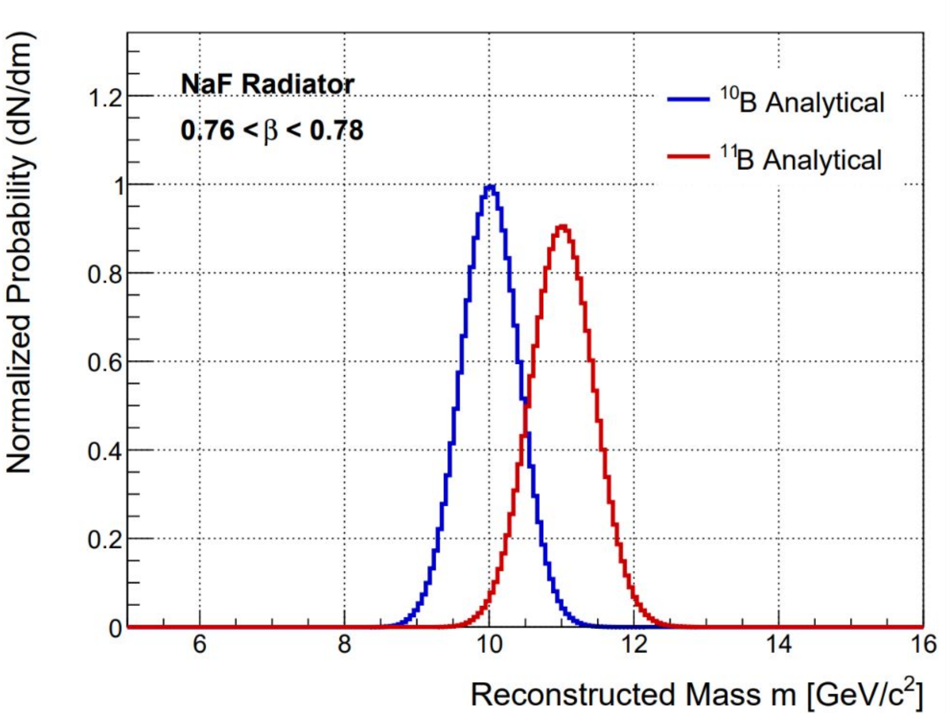

Isotopic Fraction Extraction

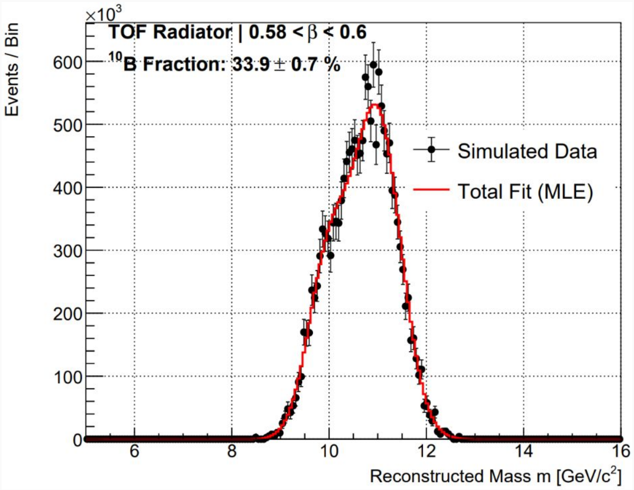

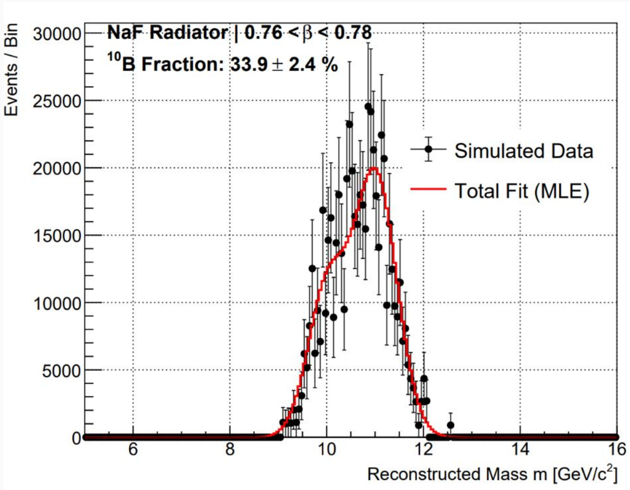

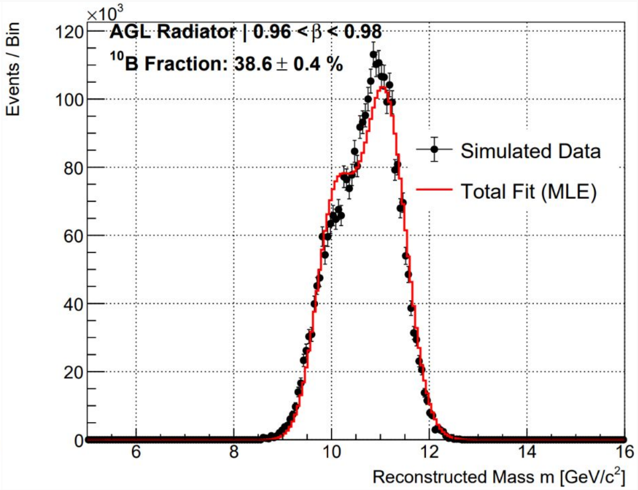

Successful Extraction: MLE fitting applied across independent velocity windows for TOF, NaF, and AGL.

Resolution Degradation: Mass reconstruction progressively worsens at higher velocities.

Kinematic Cause: As $\beta \to 1$, the γ^2 factor severely amplifies instrumental uncertainties, broadening the mass peaks.

Conclusions & Future Work

Main Conclusion: Successful resolution of the severe high-energy mass overlap using Bayesian Analytical Templates and MLE fitting (RooFit). The dual-language architecture effectively cross-validated the instrumental modeling of the TOF and RICH subsystems.

Cosmic Flux Refinement: Replacement of the generic power-law with the official AMS-02 Smoothly Broken Power Law (SBPL) parameterization, alongside the introduction of solar modulation (Fisk approximation) for low rigidities.

Dynamic Geomagnetic Filter: Implementation of continuous local cutoff rigidity calculations, correlating ISS orbital coordinates with updated magnetospheric models (IGRF).

True Trajectory Physics: Abandonment of the rectilinear approximation by integrating the true magnetic deflection for exact geometric acceptance and time-of-flight calculations.

Thank You / Q&A